Asian Journal of Chemistry; Vol. 38, No. 1 (2026), 234-242
ASIAN JOURNAL OF CHEMISTRY
https://doi.org/10.14233/ajchem.2026.34703

Fe_3O_4@SiO_2@$(CH_2)_3$@4-(2-Aminoethyl)morpholine as a Reusable Magnetic Organocatalyst for Synthesis of Pyrano[3,2-*c*]chromene Derivatives Along with Docking Study

LEILA AMIRI-ZIRTOL[1], LEILA EMAMI[1] and SOGHRA KHABNADIDEH[1,2,*]

[1]Pharmaceutical Sciences Research Center, Faculty of Pharmacy, Shiraz University, Iran
[2]Department of Medicinal Chemistry, Faculty of Pharmacy, Shiraz University of Medical Sciences, Shiraz, Iran

*Corresponding author: Fax: +98 71 32424126; Tel: +98 71 32424127-8; E-mail: khabns@sums.ac.ir

Received: 16 August 2025 *Accepted*: 18 December 2025 *Published online*: 31 December 2025 AJC-22243

Pyrano[3,2-*c*]chromene derivatives, as an important category of heterocyclic compounds, have received much attention due to their various biological activities. Different synthetic methods using various catalysts have been reported for the synthesis of these compounds. Here, a green, magnetically separable catalyst functionalized with nitrogen-containing groups was used for the synthesis of a series of pyrano[3,2-*c*]chromene derivatives. The target compounds were synthesized by employing the catalytic activity of the previously synthesized composite under environmentally friendly and mild conditions. The reaction proceeded efficiently in a water/ethanol mixture within a short time and resulted in high product yields. A multicomponent reaction was used to synthesize pyrano[3,2-*c*]chromene derivatives from malononitrile, 4-hydroxycoumarin and various aldehydes. The purity of the final compounds was checked by melting point determination and comparison with literature values. Since pyrano[3,2-*c*]chromene derivatives are proposed as potential inhibitors of DNA topoisomerases, especially TOPII, in the second part of this study, a computational study was performed targeting the DNA-TOPII complex. The results revealed that some of the synthesized compounds are known to inhibit topoisomerases, supporting their role as promising anticancer agents.

Keywords: Pyrano[3,2-*c*]chromene, Magnetically catalyst, Docking, Topoisomerase.

INTRODUCTION

To date, a wide range of substances, including organic compounds, proteins, enzymes and certain naturally occurring materials, have been successfully employed as organocatalysts. The exploration of organocatalysts, small organic molecules capable of enhancing reaction efficiency has emerged as a rapidly growing field of interest among researchers [1,2]. One of the main motivations for the development of novel organocatalyst systems lies in their potential to align organic synthesis with the principles of green chemistry, particularly due to their metal-free nature [3]. In contrast to metal-based catalysts, organocatalysts are typically non-toxic, cost-effective and exhibit excellent stability under ambient conditions, including exposure to air and moisture [4]. Moreover, their accessibility and, in some cases, low cost make them highly practical for sustainable applications. An additional advantage is their reusability without requiring extensive post-reaction purification, which further enhances their environmental compatibility [5-11].

Small organic molecules such as pyridine, proline and morpholine serve as representative examples of organocatalysts [12]. Among these, 2-morpholinoethanamine a morpholine derivative exhibits notable nucleophilic activity at its nitrogen center. This compound has proven to be an effective organocatalyst, demonstrating significant catalytic performance across a variety of organic transformations, particularly in acylation reactions [11,13]. On the other hand, multicomponent reactions are highly attractive since they proceed in a single step, require minimal time and expense and eliminate the need to isolate or purify intermediate species [14,15].

Pyrano[3,2-*c*]chromene derivatives represent a class of compounds with diverse and significant biological activities such as anticancer [16], antiviral and antimicrobial [17], anti-inflammatory, anti-HIV and antidiabetic [18] and antiangiogenesis activities [19]. Owing to their pharmacological relevance, considerable research efforts have been dedicated to the development of efficient synthetic methods for their preparation. A novel organocatalyst, Fe_3O_4@SiO_2@$(CH_2)_3$@4-(2-aminoethyl)morpholine, was synthesized in previous work,

demonstrating sufficient basic strength. The catalytic potency of this new compound was evaluated for the synthesis of polyhydroquinoline derivatives [20]. Based the catalyst's success in promoting polyhydroquinoline synthesis, the present study aims to assess its effectiveness in the synthesis of pyrano[3,2-*c*]-chromene derivatives. The catalyst offers several advantages, including strong basicity, magnetic properties, recyclability, and efficacy in organic reactions.

Although direct studies on pyrano[3,2-*c*]chromene derivatives as topoisomerase inhibitors are limited, structurally related heterocyclic compounds, such as quinoline and pyranoquinoline derivatives, have demonstrated potent topoisomerase inhibition and anticancer activity [21-24]. Besides, some chromene derivatives have been reported as active cytotoxic agents, affecting cell cycle progression, induced apoptosis in human cancer cell lines and inhibition of the topoisomerase enzyme [25]. Topoisomerase enzymes are crucial enzymes involved in DNA replication, chromosomal segregation, transcription and recombination. They exist in two classes: Topoisomerase I (TOPI) and topoisomerase II (TOPII). Camptothecin, topotecan and irinotecan target TOPI, while TOPII inhibitors like the anthracycline-based drug doxorubicin cause cytotoxic DNA double-strand breaks. Although these topo-active drugs are awfully effective and utilized to treat a wide variety of cancers, they face the common difficulty of resistance development in tumor cells, demanding novel approaches [26]. Given the structural similarity and the known biological activities of related scaffolds, it is reasonable to propose that pyrano[3,2-*c*]chromene derivatives could target topoisomerase enzymes, particularly TOPII, as part of their mechanism of action. This hypothesis is supported by molecular docking and biological evaluation studies of analogous compounds showing effective binding and inhibition of topoisomerases [27,28]. Thus, in the second part of this work, based on current literature and related compound classes, the molecular docking studies were applied against DNA topoisomerases inhibitors. Although the current study is limited to computational analysis, the potential anticancer activity of synthesized pyrano[3,2-*c*]chromene derivatives is strongly supported by experimental evidence from structurally analogous compounds. For instance, El-Agrody *et al.* [18] demonstrated significant *in vitro* cytotoxic effects for similar pyrano[3,2-*c*]chromene derivatives against various cancer cell lines using the MTT assay. Furthermore, Cholayil Palapetta *et al.* [27] synthesized closely related dihydropyrano-[3,2-*c*]chromene derivatives and confirmed their promising anticancer activity *in vitro* alongside favourable molecular docking results against cancer-related targets [27]. The existing literature provides a solid foundation for the hypothesis that the title compounds should undergo further experimental biological evaluation.

EXPERIMENTAL

All the starting materials, solvents and reagents were procured from Merck and Sigma-Aldrich, USA. Fe_3O_4@SiO_2@$(CH_2)_3$@4-(2-aminoethyl)morpholine was synthesized in several steps according to the procedures reported in previous studies [20].

Preparation of Fe_3O_4 nanoparticles: In the first step, red mud was treated with 0.2 M HCl at room temperature for 2 h to remove calcium. The pretreated red mud was then leached with 3 M HCl at 95 ºC for 2 h to eliminate silicon. Ammonia (25% solution) and 3 M NaOH were added to the resulting chloride solution to adjust the pH to 9.5 ± 0.5 and 13.5 ± 0.5, respectively, facilitating the separation of aluminum from the iron hydroxide gel ($Fe(OH)_3$). The $Fe(OH)_3$ precipitate was subsequently dissolved in 3 M HCl to prepare the chloride solution and the Fe^{2+}/Fe^{3+} molar ratio was adjusted to 2:3 by adding a calculated amount of $FeSO_4$. A black Fe_3O_4 precipitate was formed by adding 25% ammonia and adjusting the pH to 11 under vigorous stirring at 85 ºC, followed by aging for 20 min at the same temperature. The nanoparticles were washed repeatedly with deionized water and ethanol until neutral pH was achieved, dried at 105 ºC for 8 h and finally calcined at 350 ºC for 2 h to obtain Fe_3O_4 magnetic nanoparticles [29].

Preparation of Fe_3O_4@SiO_2: In this step, core-shell Fe_3O_4@SiO_2 was synthesized following the procedures reported in previous studies. Fe_3O_4 (1.0 g) was dispersed in 20 mL of ethanol/water under ultrasonication. Tetraethyl orthosilicate (TEOS, 3 mL) and aqueous ammonia (3 mL) were added and the mixture was refluxed under N_2 atmosphere at 60 ºC for 12 h. The product was separated magnetically, washed with hot ethanol and dried at 50 ºC for 6 h [30].

Preparation of Fe_3O_4@$SiO_2(CH_2)_3$–Cl nanoparticles: Fe_3O_4@SiO_2 (0.50 g) was dispersed in 40 mL ethanol for 30 min, after which (3-chloropropyl)trimethoxysilane (1 mL) was added dropwise. The mixture was refluxed under nitrogen for 6 h. The resulting Fe_3O_4@$SiO_2(CH_2)_3$–Cl nanoparticles were magnetically separated, washed with ethanol and dried at 70 ºC for 6 h.

Preparation of nanocatalyst Fe_3O_4@$SiO_2(CH_3)_3$@4-(2-aminoethyl)morpholine: Fe_3O_4@$SiO_2(CH_3)_3$–Cl was synthesized according to the method we previously reported [20]. Then, Fe_3O_4@$SiO_2(CH_3)_3$–Cl (0.5 g) was ultrasonically dispersed in 100 mL of water. Next, 0.5 g of 4-(2-aminoethyl)-morpholine was introduced into the suspension and the mixture was refluxed with constant stirring for 12 h. The resulting glutamic acid-functionalized magnetic nanoparticles were then separated from the reaction medium with an external magnet, thoroughly rinsed with hot ethanol and finally dried and stored at ambient temperature [20].

General procedure for the synthesis of pyrano[3,2-*c*]-chromene derivatives: A mixture comprising malononitrile (**1**) (0.066 g, 1 mmol), 4-hydroxycoumarin (**2**) (0.162 g, 1 mmol) and aryl aldehydes (**3**) (1 mmol), was stirred in a 50 mL round-bottom flask containing an EtOH/H_2O (1:1, v/v) along with 0.04 g of catalyst. The progress of the reaction was monitored by TLC. Upon completion, the catalyst was separated from the reaction mixture *via* an external magnet. As the mixture cooled to room temperature, the desired products **4a-j** precipitated out and was subsequently purified through recrystallization using ethanol (**Scheme-I**).

Molecular docking: To investigate the binding interactions and modes between the synthesized derivatives and DNA-TOPII, molecular docking simulations were carried out. Initially, the complexes were prepared by assigning Gasteiger

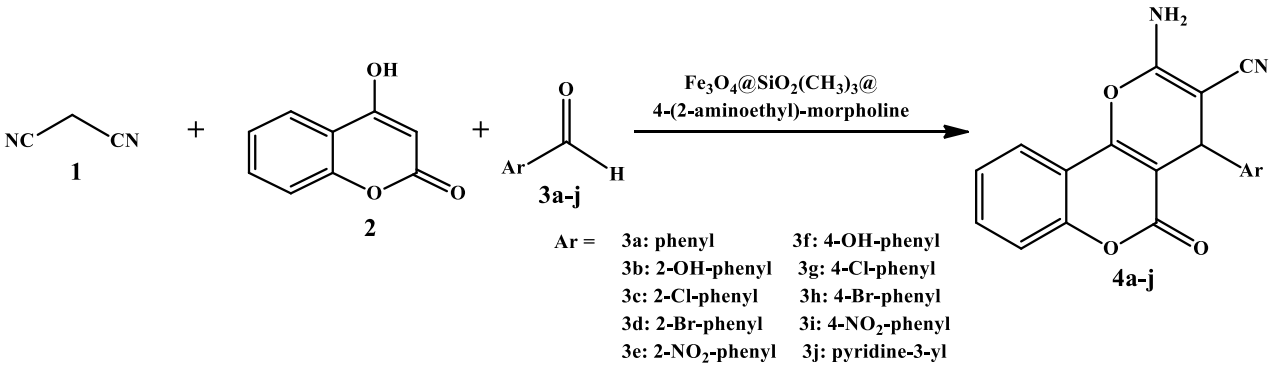

Scheme-I: Synthesis of pyrano[3,2-*c*]chromene derivatives

charges and merging nonpolar hydrogen atoms using AutoDock Tools (ADT) version 4.0. The prepared structures were then saved in the PDBQT file format for docking. The three-dimensional crystal structure of DNA-TOPII (PDB ID: 5gwk) was retrieved from the Protein Data Bank (www.rcsb.org). Prior to docking, the protein structure was cleaned by removing water molecules and ions and subsequently converted into the PDBQT format. For each ligand-DNA-TOPII complex, 50 independent docking runs were executed. The conformation exhibiting the lowest binding free energy from the most populated cluster was selected and saved in PDBQT format. A grid box with dimensions of 126 × 90 × 106 points and a center at (x = 28.70, y = -38.695, z = -60.24) was defined using the default parameters. In the self-docking validation experiment, the root-mean-square deviation (RMSD) was calculated to be 0.95 Å. This result confirms the validity of the docking protocol, as the RMSD value is below the accepted threshold of 2.0 Å. Finally, docking outcomes were thoroughly analyzed using AutoDock Tools (ADT) 4.0 to elucidate the key intermolecular interactions and binding affinities.

RESULTS AND DISCUSSION

4-(2-Aminoethyl)-morpholine molecule was immobilized onto the surface of Fe_3O_4@SiO_2@Si$(CH_3)_3$–Cl in ethanol under reflux conditions, following a previously reported procedure. The resulting composite demonstrated notable basicity, attributed to the presence of amine functional groups. The structural characteristics of the composite were further verified through FT-IR, SEM, XRD and VSM analyses.

Catalyst identification: The FT-IR spectrum of Fe_3O_4@SiO_2@$(CH_2)_3$@4-(2-aminoethyl)morpholine is illustrated in Fig. 1. The spectral changes verify the successful incorporation of 2-morpholinoethanamine onto Fe_3O_4@SiO_2@$(CH_3)_3$–Cl surface. The absorption band at 3413 cm^{-1} corresponds to NH and OH stretching vibrations. The distinct CH_2 peaks at 2923 cm^{-1} further confirm the presence of 2-morpholinoethanamine. Furthermore, the characteristic bands at 1093 and 584 cm^{-1} indicate the existence of Fe_3O_4@SiO_2.

The X-ray diffraction (XRD) patterns of the synthesized nanocomposite are illustrated in Fig. 2, where the diffraction intensity is plotted against the 2θ angle. The characteristic diffraction peaks observed at 2θ values of 30.79º, 36.8º, 44.5º, 54.8º, 58.2º and 63.44º are in good agreement with the standard diffraction data of magnetite (Fe_3O_4) [31], thereby

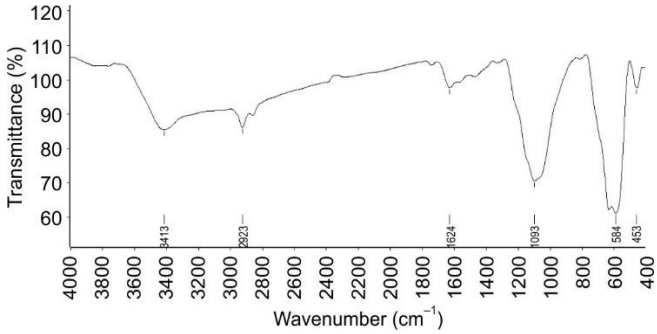

Fig. 1. FT-IR spectrum of Fe_3O_4@SiO_2@$(CH_2)_3$@4-(2-aminoethyl)-morpholine

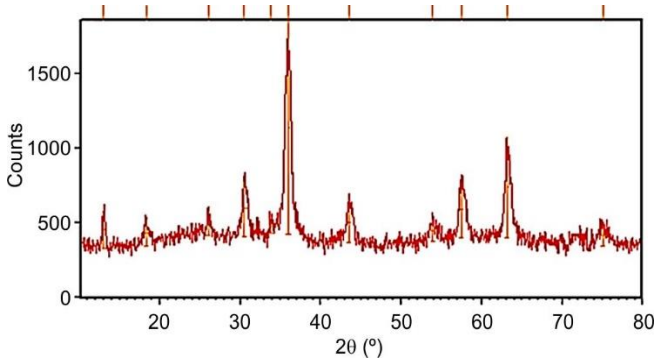

Fig. 2. XRD spectrum of Fe_3O_4@SiO_2@$(CH_2)_3$@4-(2-aminoethyl)-morpholine

confirming the successful synthesis of the magnetic phase. Importantly, these reflections are clearly retained in the XRD pattern of Fe_3O_4@SiO_2@$(CH_2)_3$@4-(2-aminoethyl)morpholine nanocomposite, indicating that the crystalline structure of Fe_3O_4 remains stable after surface functionalization.

The morphology and structural characteristics of the synthesized nanocomposite are shown in Fig. 3. Panels a-b display the FE-SEM images, which reveal that the particles exhibit a well-defined spherical shape with high uniformity. The micrographs clearly demonstrate that the nanoparticles are homogeneously distributed without significant aggregation. Furthermore, as depicted in panel b, the average particle size is in the range of 20-30 nm, confirming the nanoscale dimension and uniform arrangement of the particles within the composite matrix.

Fig. 4 shows the VSM results, indicating the magnetic strength of the composite. The magnetic strength ranges from

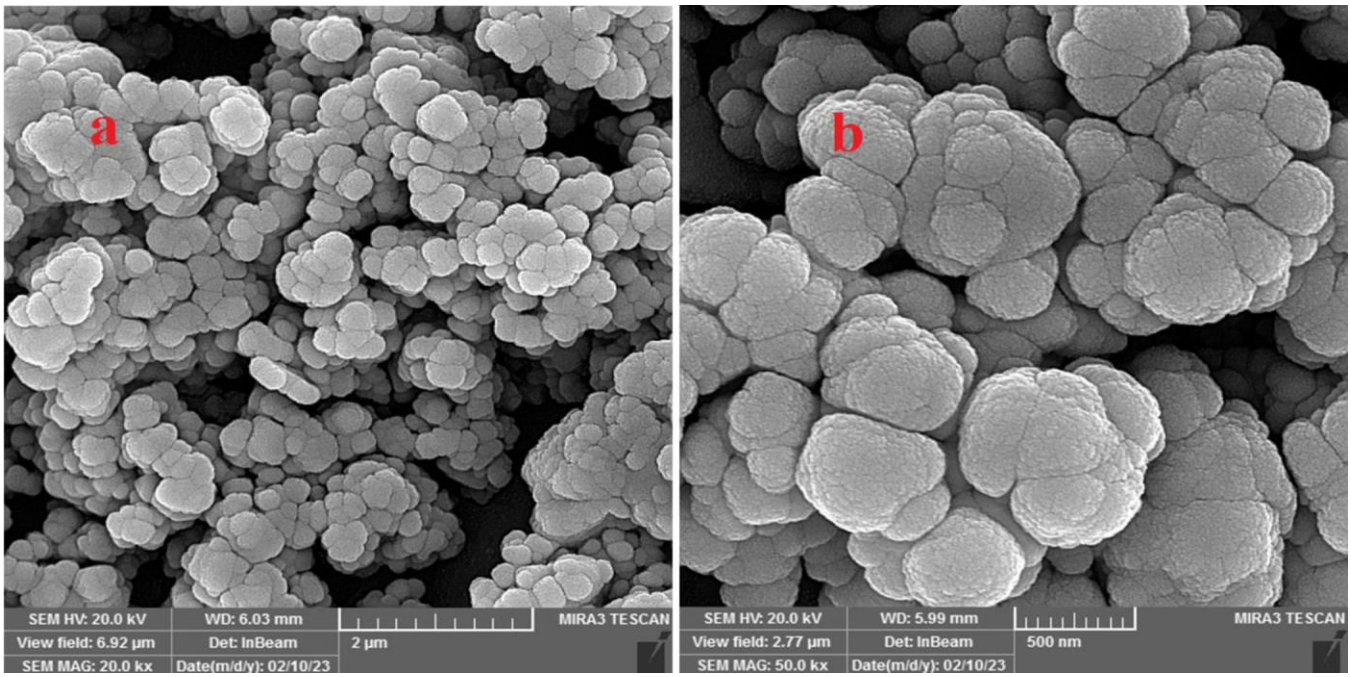

Fig. 3. FE-SEM image of Fe_3O_4@SiO_2@$(CH_2)_3$@4-(2-aminoethyl)-morpholine

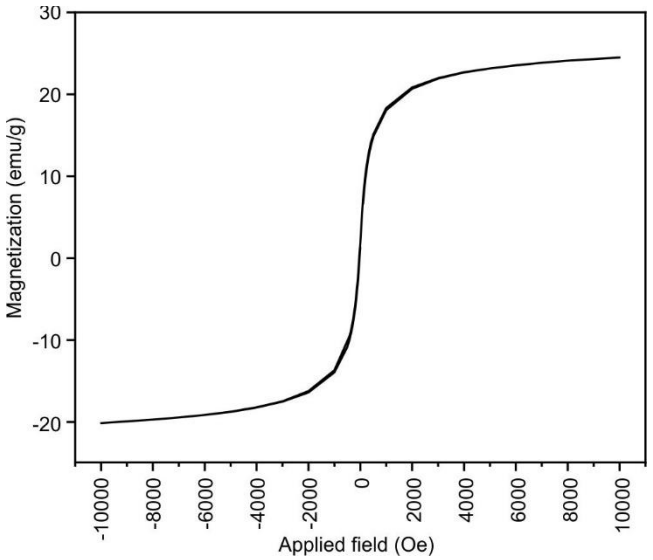

Fig. 4. VSM spectrrum of Fe_3O_4@SiO_2@$(CH_2)_3$@4-(2-aminoethyl)-morpholine

-20 to 20 emu g^{-1}, confirming its good magnetic qualities. The curve demonstrates that Fe_3O_4@SiO_2@$(CH_2)_3$@4-(2-aminoethyl)morpholine is intrinsically magnetic, with sufficient magnetic susceptibility for facile separation from reaction media using an external magnet. This convenient separation and recovery method underscores the potential of composite in catalytic applications.

Optimization of the reaction conditions: Following preparation of the catalyst, it was applied in the synthesis of pyrano[3,2-*c*]chromene derivatives. To establish the optimal conditions for this transformation, a series of experiments were conducted using a model reaction between malononitrile (**1**), 4-hydroxycoumarin (**2**) and 4-nitrobenzaldehyde (**3i**) to obtain **4i**. Initially, the reaction was examined under catalyst-free conditions, followed by trials using Fe_3O_4, 4-(2-aminoethyl)morpholine and Fe_3O_4@SiO_2@$(CH_2)_3$@4-(2-aminoethyl)morpholine (0.04 g) as catalysts. The comparative results, obtained from three independent experiments, clearly demonstrated the superior efficiency of morpholine-functionalized magnetic nanocatalyst, highlighting its potential as a robust heterogeneous catalyst for this transformation. The comparison of reaction yields across these setups clearly demonstrated the superior performance of the morpholine-based magnetic nanocatalyst, confirming its potential as an efficient heterogeneous catalyst for this transformation (Table-1, entries 1-4). Subsequently, the role of solvent as a critical factor influencing reaction efficiency and environmental safety was investigated. A variety of solvents, including ethanol, water, solvent-free condition and mixture of water and ethanol were tested. Among these, mixture of water and ethanol (1:1) emerged as the most effective medium. The best outcome, with yields reported as mean ± SD (Table-1, entries 4-7). The effect of temperature on the reaction outcome was also evaluated by conducting the reaction at room temperature, 60 °C and under reflux. The optimal temperature was determined to be 60 °C, providing a balance between reaction rate and product yield (Table-1, entries 7-9). Finally, to optimize catalyst loading, several trials were performed with different amounts of nanocatalyst (Table-1, entries 9-12). It was concluded that 0.03 g of Fe_3O_4@SiO_2@$(CH_2)_3$@4-(2-aminoethyl)-morpholine offered the most favourable results. The results indicated that 0.03 g of nanocatalyst offered the most favourable performance (mean yield: 98% ± 2 SD). Therefore, the optimal conditions for this reaction were identified as using 0.03 g of catalyst in 1:1 EtOH/H_2O system at 60 °C (Table-1, entry 10).

Catalytic activity: Following optimization of the model reaction and identification of the most favourable reaction conditions, a series of target pyrano[3,2-*c*]chromene deriva-

TABLE-1
OPTIMIZATION OF THE REACTION CONDITIONS FOR SYNTHESIS OF **4i**

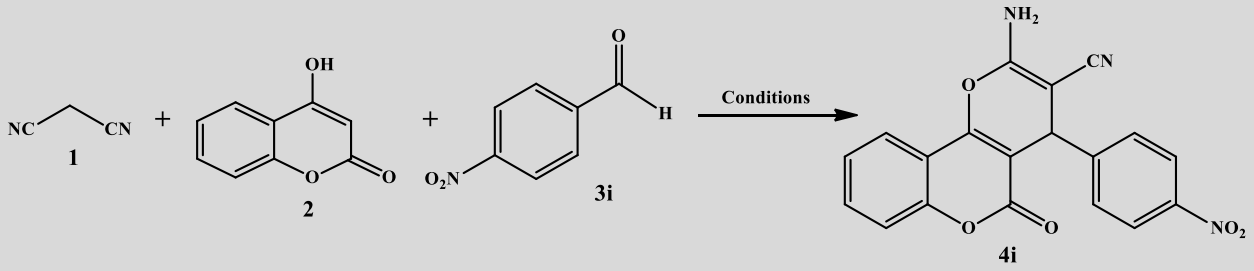

Entry	Catalyst	g	Temp. (ºC)	Solvent	Time (min)	Yield[b] (%)
1	–	–	60	EtOH	60	40 ± 5
2	Fe_3O_4	0.04	60	EtOH	45	65 ± 6
3	Mor	0.04	60	EtOH	30	83 ± 4
4	$Fe_3O_4@SiO_2@(CH_2)_3$@4-(2-Aminoethyl)-morpholine	0.04	60	EtOH	12	93 ± 2
5	$Fe_3O_4@SiO_2@(CH_2)_3$@4-(2-Aminoethyl)-morpholine	0.04	60	EtOH/H_2O (1:1)	20	93 ± 4
6	$Fe_3O_4@SiO_2@(CH_2)_3$@4-(2-Aminoethyl)-morpholine	0.04	60	Solvent-free	15	93 ± 2
7	$Fe_3O_4@SiO_2@(CH_2)_3$@4-(2-Aminoethyl)-morpholine	0.04	60	H_2O	30	80 ± 5
8	$Fe_3O_4@SiO_2@(CH_2)_3$@4-(2-Aminoethyl)-morpholine	0.04	r.t.	EtOH/H_2O (1:1)	30	85 ± 2
9	$Fe_3O_4@SiO_2@(CH_2)_3$@4-(2-Aminoethyl)-morpholine	0.04	Reflux	EtOH/H_2O (1:1)	12	95 ± 5
10	$Fe_3O_4@SiO_2@(CH_2)_3$@4-(2-Aminoethyl)-morpholine	0.03	60	EtOH/H_2O (1:1)	12	98 ± 2
11	$Fe_3O_4@SiO_2@(CH_2)_3$@4-(2-Aminoethyl)-morpholine	0.02	60	EtOH/H_2O (1:1)	18	83 ± 7
12	$Fe_3O_4@SiO_2@(CH_2)_3$@4-(2-Aminoethyl)-morpholine	0.01	60	EtOH/H_2O (1:1)	30	65 ± 3

[a]Optimized reaction conditions: 4-Nitrobenzaldehyde (1 mmol), malononitrile (1 mmol) and 4-Hydroxycoumarin (1 mmol), [b]Isolated yields based on the average of three independent experiments; values represent mean ± standard deviation based on three independent experiments.

tives were successfully synthesized. A summary of the synthesized compounds and their corresponding yields is shown in Table-2. The enhanced reactivity of aldehydes bearing electron-withdrawing substituents can be attributed to increased electrophilicity of the carbonyl carbon, which facilitates more efficient interaction with the catalytic species and promotes higher product yields.

TABLE-2
SYNTHESIS OF PYRANO[3,2-*c*]CHROMENES UNDER OPTIMIZED CONDITIONS[b]

Entry	Time (min)	Yield (%)[b]	m.p. (ºC)	
			Found	Reported
4a	20	95	150-151	147-150 [Ref. 32]
4b	18	95	267-270	267-270 [Ref. 33]
4c	12	95	269-271	273-275 [Ref. 33]
4d	12	95	297-298	294-296 [Ref. 34]
4e	14	98	255-259	258-260 [Ref. 34]
4f	18	93	270-272	271-273 [Ref. 32]
4g	14	98	187-189	189-192 [Ref. 32]
4h	16	98	250-254	252-254 [Ref. 34]
4i	12	98	244-247	247-249 [Ref. 32]
4j	12	95	251-255	250-252 [Ref. 32]

Mechanism: A proposed mechanism for synthesis of pyrano[3,2-*c*]chromenes derivatives in the presence of $Fe_3O_4@SiO_2@(CH_2)_3$@4-(2-aminoethyl)morpholine is shown in Fig. 5. Based on the research carried out to date on the synthesis of chromene derivatives in the presence of basic catalysts, the following reaction mechanism is suggested [33,35,36].

The reaction is initiated by the deprotonation of malononitrile, whose α-hydrogens exhibit strong acidity and are readily abstracted by morpholine, producing a stabilized carbanion through the electron-withdrawing influence of the two cyano substituents. This carbanion subsequently engages in a Knoevenagel condensation with the aldehyde, affording an α,β-unsaturated nitrile intermediate. The latter then undergoes a Michael addition with 4-hydroxycoumarin, which is followed by intramolecular cyclization and dehydration to furnish the pyrano[3,2-*c*]chromene framework. The process concludes with a tautomerization or structural rearrangement that stabilizes the final product. Overall, this multicomponent sequence provides a pyrano[3,2-*c*]chromene core, wherein the nature of the aldehyde commands the aromatic substitution pattern.

Recyclability of the catalyst: The model reaction was performed to investigate the recyclability of $Fe_3O_4@SiO_2@(CH_2)_3$@4-(2-aminoethyl)-morpholine. After completion, the catalyst was separated by simple filtration, thoroughly washed with hot ethanol and dried at room temperature prior to reuse in subsequent cycles. Remarkably, the catalyst retained its catalytic efficiency over six consecutive runs without any significant loss of activity (Fig. 6). In addition, FT-IR analyses of the synthesized composite before and after the reaction were conducted to verify the structural stability of the catalyst. As shown in Fig. 7, the identical spectra obtained in both cases confirm that the structural framework of the catalyst remained unchanged after the reaction process.

Molecular docking: Molecular docking simulations were performed to predict the binding modes and affinities of the synthesized pyrano[3,2-*c*]chromene derivatives against the DNA-topoisomerase IIα (DNA-TOPIIα) complex (PDB ID: 5GWK), a well-established anticancer target. The reliability of the docking protocol was first validated by a self-docking experiment. The crystallographic ligand (EVP) was re-docked

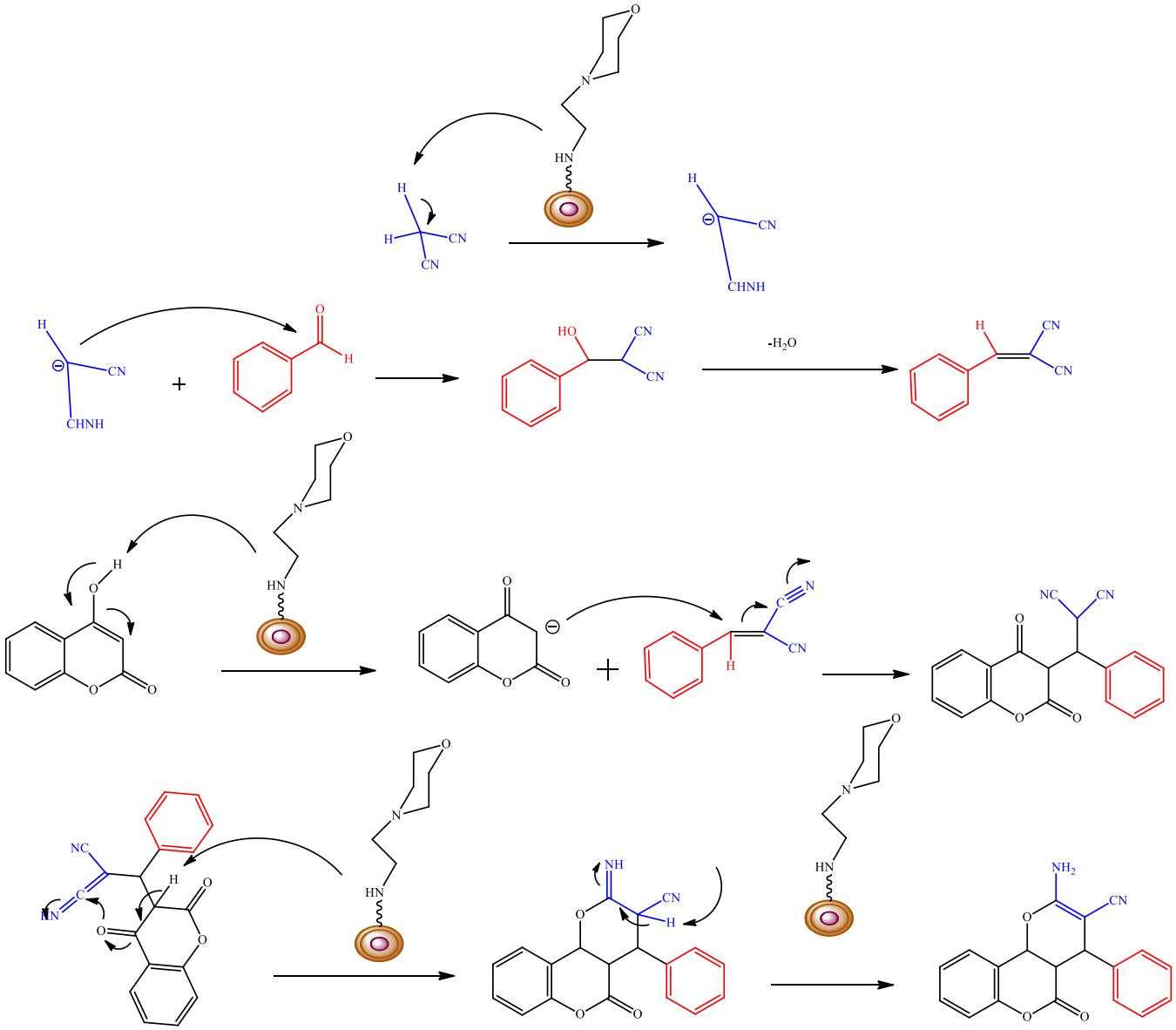

Fig. 5. The proposed mechanism for the reaction in the presence of Fe_3O_4@SiO_2@$(CH_2)_3$@4-(2-aminoethyl)morpholine

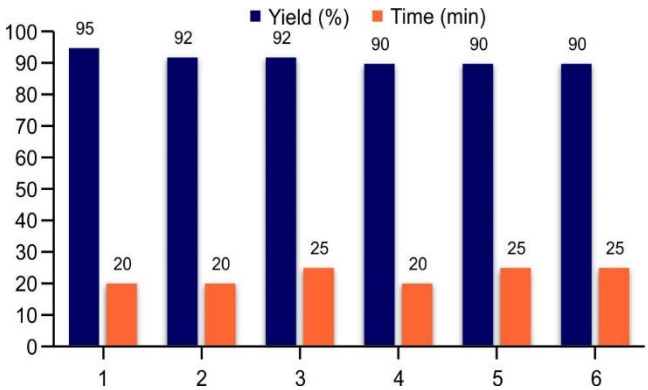

Fig. 6. Catalyst recycling experiment of Fe_3O_4@SiO_2@$(CH_2)_3$@4-(2-aminoethyl)morpholine in synthesis of **4i**

into its original binding site. The resulting root-mean-square deviation (RMSD) between the docked pose and the original conformation was 0.95 Å, which is below the accepted threshold of 2.0 Å, confirming the accuracy and validity of the docking parameters.

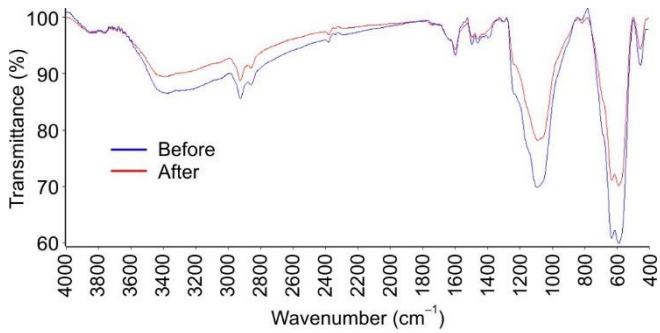

Fig. 7. FT-IR spectra of Fe_3O_4@SiO_2@$(CH_2)_3$@4-(2-aminoethyl)-morpholine before (blue) and after (red) recycling

The binding free energies (ΔG) for the synthesized compounds ranged from -7.3 to -9.2 kcal/mol. To contextualize the potential inhibitory strength of these novel compounds,

their performance was benchmarked against doxorubicin, a potent classic TOPII inhibitor clinically used in cancer chemotherapy. Docking analysis revealed that doxorubicin yielded a significantly favourable binding energy of -10.2 kcal/mol with the DNA-TOPIIα complex, forming characteristic hydrogen bonds and stacking interactions within the active site, as illustrated in Fig. 8.

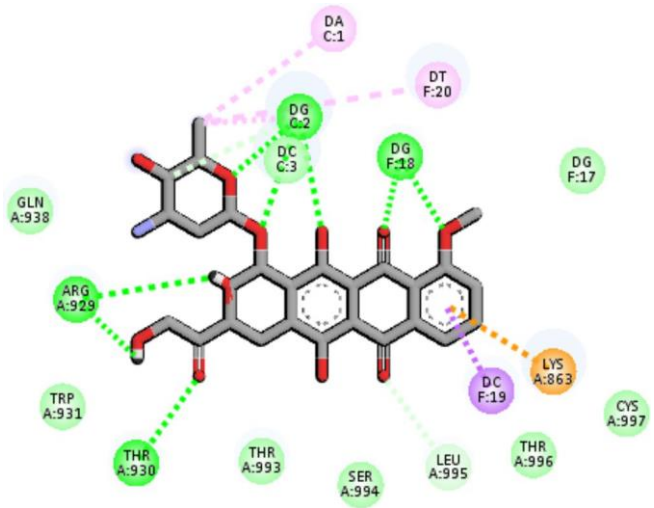

Fig. 8. Two-dimensional and three-dimensional binding interactions of the standard inhibitor, doxorubicin, within the active site of the DNA-Topo IIα complex (PDB: 5GWK)

Among the synthesized derivatives, compound **4e** exhibited the strongest theoretical binding affinity, with a calculated energy of -9.2 kcal/mol. Analysis of its binding mode, depicted in Fig. 9, showed that compound **4e** fits snugly into the active site. Key interactions included hydrogen bonds between its carbonyl and oxygen atoms with DNA bases DG2 and DT20 and its amino group with amino acid residues Thr920 and Val928. Additional stability was provided by a π–π stacking interaction with Leu995. This interaction profile suggests that compound **4e** has a high potential to intercalate and disrupt the DNA-TOPIIα interface, thereby inhibiting the enzyme's function.

In contrast, compound **4f**, with the lowest binding energy (-7.3 kcal/mol) in the series, demonstrated a weaker and less favourable interaction profile. As shown in Fig. 10, its binding was primarily stabilized by only a single hydrogen bond with Glu839 and a π–π interaction with Arg673, lacking significant contact with the DNA bases, which is crucial for effective TOPII inhibition.

While the binding energy of the most promising compound, **4e** (-9.2 kcal/mol), is slightly less favourable than that of doxorubicin (-10.2 kcal/mol), it still indicates a strong and specific binding affinity. Furthermore, the ability of compound **4e** to interact with both DNA bases and key amino acid residues mirrors the mechanism of known TOPII inhibitors. This computational evidence, supported by studies on structurally related chromene derivatives exhibiting potent topoisomerase II inhibition and anticancer activity [33,35], strongly suggests that pyrano[3,2-*c*]chromene derivatives, particularly compound **4e**, are promising candidates for further development as potential anticancer agents targeting TOPII. The docking results suggesting inhibition of DNA-topoisomerase IIα align with the reported mechanism of action for related chromene derivatives. El-Mawgoud *et al.* [25] identified chromene-based compounds as multi-target inhibitors, including potent topoisomerase II inhibition, which was

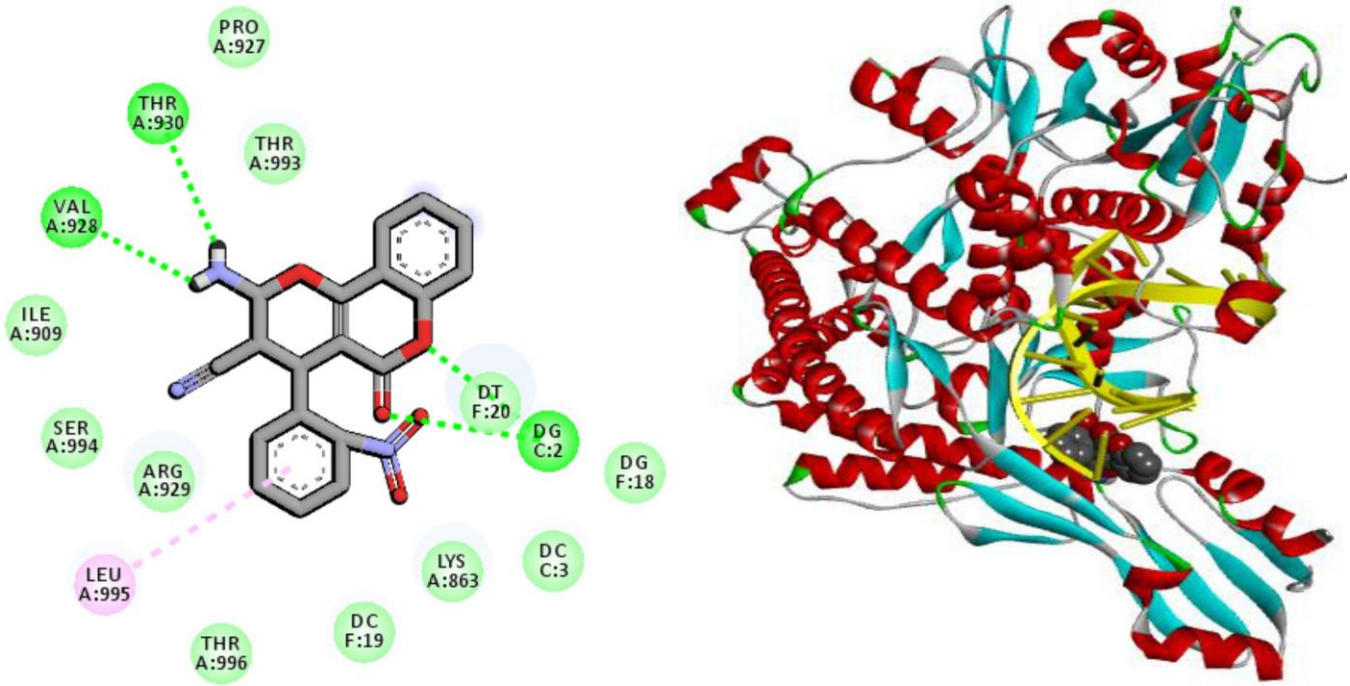

Fig. 9. Binding interactions of the most potent synthesized compound, **4e** (ΔG = -9.2 kcal/mol), within the DNA-Topo IIα binding site. Key hydrogen bonds (green dashed lines) with Thr920, Val928, DG2 and DT20, along with a π–π stacking interaction with Leu995, are shown

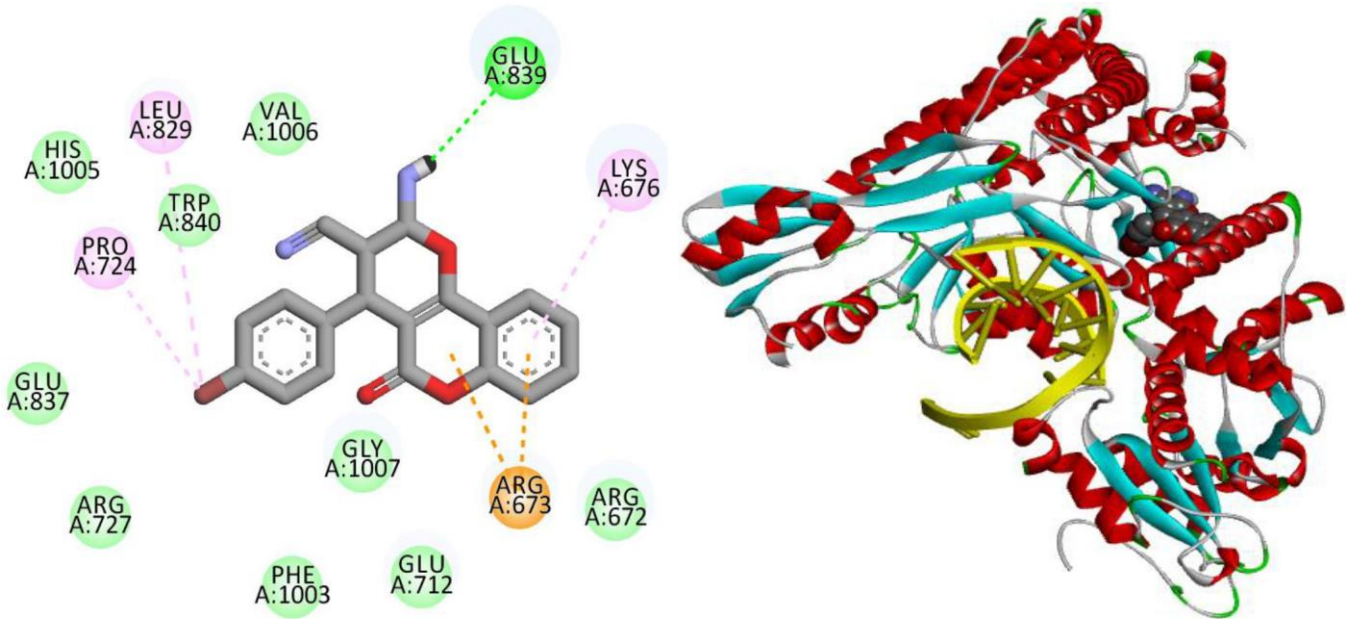

Fig. 10. Binding mode of the least potent compound, **4f** (ΔG = -7.3 kcal/mol); (a) 2D schematic showing a hydrogen bond with Glu839 and a π–π stacking with Arg673; (b) 3D view of the docking pose

correlated with their anticancer efficacy. This consistency between our computational predictions and the experimental findings for analogous scaffolds provides a compelling rationale for considering pyrano[3,2-*c*]chromene derivatives as prospective topoisomerase II inhibitors with anticancer potential.

Conclusion

In this study, a nano-heterogeneous organocatalyst incorporating a small organic molecule with strong catalytic activity was employed. Utilizing this synthesized catalyst, a series of pyrano[3,2-*c*]chromene derivatives were successfully prepared under mild conditions, achieving high yields within relatively short reaction times. Different pyrano[3,2-*c*]chromene analogues holding electron donating and withdrawing groups at *ortho*- or *para*-positions were effectively synthesized. The novelty of this work lies in the design of a bifunctional, morpholine-grafted magnetic nanocatalyst that combines strong catalytic activity with excellent recyclability due to its silica-protected magnetic core. The key advantages of the presented protocol include its green credentials (using a water/ethanol solvent mixture), operational simplicity (facilitated by magnetic separation) and high efficiency across a diverse range of substrates. Subsequently, molecular docking studies were carried out on the synthesized compounds against the DNA-topoisomerase IIα (DNA-TOPIIα) complex, given the enzyme's crucial role in cancer cell proliferation. The results identified compound **4e** as a promising inhibitor, revealing its effective binding within the active site through significant interactions with key amino acid residues (Thr920, Val928) and DNA bases (DG2, DT20). While experimental validation remains a necessary next step, the theoretical potential of these compounds is strongly supported by compelling evidence from structurally analogous compounds in the literature. Acknowledging the limitations of this study, the primary constraint is the lack of *in vitro* or *in vivo* biological data to experimentally corroborate the docking predictions at this stage. Therefore, the future perspectives will be directed toward conducting such essential biological assays, including MTT assays for cytotoxicity and topoisomerase II enzyme inhibition studies, to validate the potential of these compounds as anticancer agents. Further exploration of the catalyst's applicability to other multicomponent reactions is also planned.

ACKNOWLEDGEMENTS

Financial assistance from the Shiraz University of Medical Sciences (grant number 28071) is gratefully acknowledged.

CONFLICT OF INTEREST

The authors declare that there is no conflict of interests regarding the publication of this article.

DECLARATION OF AI-ASSISTED TECHNOLOGIES

The authors declare that no AI tools were used in the preparation or writing of this research/review article.

REFERENCES

1. M.P. van Der Helm, B. Klemm and R. Eelkema, *Nat. Rev. Chem.*, **3**, 491 (2019); https://doi.org/10.1038/s41570-019-0116-0
2. M. Ganesan, J. Krogman, T. Konovalova and L.L. Diaz, *ChemRxiv* (2023); https://doi.org/10.26434/chemrxiv-2023-v30kj-v2
3. S. Zlotin, K. Egorova, V. Ananikov, A. Akulov, M. Varaksin, O. Chupakhin, V.N. Charushin, K.P. Bryliakov, A.D. Averin, I.P. Beletskaya, E.L. Dolengovski, Y.H. Budnikova, O.G. Sinyashin, Z.N. Gafurov, A.O. Kantyukov, D.G. Yakhvarov, M.N. Elinson, V.G. Nenajdenko, D.A. Guk, A.V. Aksenov, A.M. Chibiryaev, N.S. Nesterov, E.A. Kozlova, O.N. Martyanov, I.A. Balova, V.N. Sorokoumov, E.K. Beloglazkina, D.A. Lemenovskii, I.Y. Chukicheva, A.V. Popov, L.L. Frolova, E.S. Izmest'ev, I.A. Dvornikova, A.V. Kutchin, D.M. Borisova, A.A. Kalinina, A.M. Muzafarov, I.V. Kuchurov, A.L. Maximov and A.V. Zolotukhina, *Russ. Chem. Rev.*, **92**, RCR5104 (2023); https://doi.org/10.59761/RCR5104

4. V. Mishra and S.C. Peter, *Chem Catal.*, **4**, 100796 (2024); https://doi.org/10.1016/j.checat.2023.100796
5. H. Zhou, Y. Zhou, H.Y. Bae, M. Leutzsch, Y. Li, C.K. De, G.-J. Cheng, and B. List, *Nature*, **605**, 84 (2022); https://doi.org/10.1038/s41586-022-04531-5
6. S. Chehab, Y. Merroun, R. Ghailane, S. Boukhris and A. Souizi, *Polycycl. Aromat. Compd.*, **43**, 4906 (2023); https://doi.org/10..1080/10406638.2022.2094421
7. P. Singh, P. Yadav, A. Mishra and S.K. Awasthi, *ACS Omega*, **5**, 4223 (2020); https://doi.org/10.1021/acsomega.9b04117
8. M. Kazemi and M. Mohammadi, *Appl. Organomet. Chem.*, **34**, e5400 (2020); https://doi.org/10.1002/aoc.5400
9. M. Kazemi, R. Ali, V. Jain, S. Ballal, M.K. Abosaoda, A. Singh, T. Krithiga, K.K. Joshi and R. Javahershenas, *RSC Adv.*, **15**, 23054 (2025); https://doi.org/10.1039/D5RA02493E
10. F. Vaghi, G. Facchetti, I. Rimoldi, M. Bottiglieri, A. Contini, M.L. Gelmi and R. Bucci, *Front Chem.*, **11**, 1233097 (2023); https://doi.org/10.3389/fchem.2023.1233097
11. P. Rai and D. Gupta, *Synth. Commun.*, **51**, 3059 (2021); https://doi.org/10.1080/00397911.2021.1968910
12. B.R. Thorat, S.N. Mali, S.S. Wavhal, D.S. Bhagat, R.M. Borade, A. Chapolikar, A. Gandhi and P. Shinde, *Comb. Chem. High Throughput Screen.*, **26**, 1108 (2023); https://doi.org/10.2174/1386207325666220720105845
13. V. Patel, T. Bambharoliya, D. Shah, D. Patel, M. Patel, U. Shah, M. Patel, S. Patel, N. Solanki, A. Mahavar, A. Nagani, H. Patel, M. Rathod, B. Bhimani, V. Bhavsar, S. Padhiyar, S. Koradia, C. Chandarana, B. Patel, R.C. Dabhi and A. Patel, *Curr. Top. Med. Chem.*, **25**, 437 (2025); https://doi.org/10.2174/0115680266305231240712104736
14. C. Wang, B. Yu, W. Li, W. Zou, H. Cong, and Y. Shen, *Mater. Today Chem.*, **25**, 100948 (2022); https://doi.org/10.1016/j.mtchem.2022.100948
15. G. Bosica and R. Abdilla, *Catalysts*, **12**, 725 (2022); https://doi.org/10.3390/catal12070725
16. A.M. El-Agrody, A.M. Fouda, M.A. Assiri, A. Mora, T.E. Ali, M.M. Alam, and M.Y. Alfaifi, *Med. Chem. Res.*, **29**, 617 (2020); https://doi.org/10.1007/s00044-019-02494-3
17. E. Farzaneh, M. Mohammadi, P. Raymand, M. Noori, S. Golestani, S. Ranjbar, Y. Ghasemi, M. Mohammadi-Khanaposhtani, M. Asadi, E. Nasli Esfahani, H. Rastegar, B. Larijani, M. Mahdavi and P. Taslimi, *Bioorg. Chem.*, **145**, 107207 (2024); https://doi.org/10.1016/j.bioorg.2024.107207
18. A.M. El-Agrody, A.M. Fouda, M.A. Assiri, A. Mora, T.E. Ali, M.M. Alam and M.Y. Alfaifi, *Med. Chem. Res.*, **29**, 617 (2020); https://doi.org/10.1007/s00044-019-02494-3
19. A. Chaudhary, K. Singh, N. Verma, S. Kumar, D. Kumar and P.P. Sharma, *Mini Rev. Med. Chem.*, **22**, 2736 (2022); https://doi.org/10.2174/1389557522666220331161636
20. L. Amiri-Zirtol, A. Yargholi, L. Emami, Z. Karimi and S. Khabnadideh, *J. Saudi Chem. Soc.*, **28**, 101922 (2024); https://doi.org/10.1016/j.jscs.2024.101922
21. B.H. Pursuwani, B.S. Bhatt, F.U. Vaidya, C. Pathak and M.N. Patel, *J. Biomol. Struct. Dyn.*, **39**, 2894 (2021); https://doi.org/10.1080/07391102.2020.1756912
22. H.K. Abd El-Mawgoud, H.A.M. Radwan, F. El-Mariah and A.M. El-Agrody, *Lett. Drug Des. Discov.*, **15**, 857 (2018); https://doi.org/10.2174/1570180814666171027160854
23. A. Zarei, S. Moradi, L. Hosseinzadeh, M.B. Salavati, F. Jalilian, M. Shahlaei, K. Sadrjavadi and H. Adibi, *J. Mol. Struct.*, **1322**, 140331 (2025); https://doi.org/10.1016/j.molstruc.2024.140331
24. D.K. Sahoo, N.P. Mishra, S. Shekh and E.E. Etim, *Chem. Zvesti*, **78**, 8045 (2024); https://doi.org/10.1007/s11696-024-03654-5
25. H.K. El-Mawgoud, A.M. Fouda, M.A. El-Nassag, A.A. Elhenawy, M.Y. Alshahrani and A.M. El-Agrody, *Chem. Biol. Interact.*, **355**, 109838 (2022); https://doi.org/10.1016/j.cbi.2022.109838
26. N.K. Sharma, A. Bahot, G. Sekar, M. Bansode, K. Khunteta, P.V. Sonar, A. Hebale, V. Salokhe and B.K. Sinha, *Cancers*, **16**, 680 (2024); https://doi.org/10.3390/cancers16040680
27. S.C. Palapetta, H. Gurusamy and S. Ganapasam, *ACS Omega*, **8**, 7415 (2023); https://doi.org/10.1021/acsomega.2c06049
28. F.S. Abu El-Azm, M.M. El-Shahawi, A.S. Elgubbi and H.M. Madkour, *Synth. Commun.*, **50**, 669 (2020); https://doi.org/10.1080/00397911.2019.1710850
29. Z. Karimi and A. Rahbar-Kelishami, *J. Mol. Liq.*, **368**, 120751 (2022); https://doi.org/10.1016/j.molliq.2022.120751
30. R. Eisavi and F. Ahmadi, *Sci. Rep.*, **12**, 11939 (2022); https://doi.org/10.1038/s41598-022-15980-3
31. N. Zarei, M.A. Zolfigol, M. Torabi and M. Yarie, *Sci. Rep.*, **13**, 9486 (2023); https://doi.org/10.1038/s41598-023-35849-3
32. L. Amiri-Zirtol and S. Khabnadideh, *ChemistrySelect*, **8**, e202204007 (2023); https://doi.org/10.1002/slct.202204007
33. L. Amiri-Zirtol, T.S. Ahooie, E. Riazimontazer, M.A. Amrollahi and B.-F. Mirjalili, *Sci. Rep.*, **13**, 17966 (2023); https://doi.org/10.1038/s41598-023-44521-9
34. S.S. Mansoor, K. Logaiya, K. Aswin and P.N. Sudhan, *J. Taibah Univ. Sci.*, **9**, 213 (2015); https://doi.org/10.1016/j.jtusci.2014.09.008
35. A. Chelihi, A.M. Tahir, R. Hassaine, I. Daoud, M. Benabdallah, A.Z. Merzouk, H. Merzouk, N. Choukchou-Braham and N. Taibi, *J. Mol. Struct.*, **1322**, 140554 (2025); https://doi.org/10.1016/j.molstruc.2024.140554
36. D. Mallah, B.B.F. Mirjalili and A. Bamoniri, *Sci. Rep.*, **13**, 6376 (2023); https://doi.org/10.1038/s41598-023-33286-w